PCCP

Cite this: *Phys. Chem. Chem. Phys.*, 2011, **13**, 16343–16348

www.rsc.org/pccp

PAPER

Electron paramagnetic resonance investigation of the electron-doped manganite $La_{1-x}Te_xMnO_3$ ($0.1 \leq x \leq 0.2$)

J. Yang,*[a] X. Rong,[b] D. Suter[c] and Y. P. Sun*[ad]

Received 3rd June 2011, Accepted 20th July 2011
DOI: 10.1039/c1cp21807g

The electron paramagnetic resonance (EPR) properties of the electron-doped manganite $La_{1-x}Te_xMnO_3$ ($0.1 \leq x \leq 0.2$) are investigated based on the data of EPR spectra, resistivity, and magnetic susceptibility. With decreasing temperature from 400 K, the EPR linewidth ΔH_{PP} decreases and passes through a minimum at T_{min}, then substantially increases with further decreasing temperature. The broadening of the EPR linewidth above T_{min} can be understood in terms of the increase in the relaxation rate of spin of e_g polarons to the lattice with increasing temperature due to the similarity between the temperature dependence of the linewidth ΔH_{pp}(T) and the conductivity $\sigma(T)$. For the samples with $x = 0.1$ and 0.15, the conductivity activation energy E_σ is comparable with the activation energy E_a deduced from the linewidth. Whereas for the $x = 0.2$ sample, there is a large difference between E_σ (0.2206 eV) and E_a (0.0874 eV).

1. Introduction

Since electron paramagnetic resonance (EPR) is a powerful probe of spin dynamics and is helpful for understanding magnetic interactions and spin correlation on a microscopic level, a number of EPR studies have been performed on colossal magnetoresistance (CMR) manganites aimed at understanding the microscopic nature of the interplay between spin and charge degrees of freedom.[1–12] EPR results on the hole-doped CMR materials with the transition from paramagnetic (PM) state to ferromagnetic (FM) state show some characteristic features as follows: (1) The EPR signals in CMR manganites are a consequence of some complex magnetic entity made of a collection of $Mn^{3+}$and Mn^{4+}ions,[3] (2) The peak-to-peak linewidth (ΔH_{PP}) is large, and (3) ΔH_{PP} shows a minimum at T_{min}, *i.e.*, with decreasing temperature, ΔH_{PP} decreases and passes through a minimum at T_{min}, then substantially increases on further decreasing temperature. However, a considerable amount of controversy exists regarding the interpretation of the ΔH_{PP} dependence on temperature for $T \geq T_{min}$.[1,2,4,5,7,8] On the whole, most of the EPR investigations have been focused on the hole-doped manganites. In contrast, there are few EPR reports on the electron-doped manganites.[13–15] Moreover, the investigations on the electron-doped manganties mostly focus on the $Ca_{1-x}(La/Ce)_xMnO_3$ systems with PM-antiferromagnetic transition in which there is a mixture of Mn^{3+}/Mn^{4+}ions and the content of $Mn^{4+}$is large than that of Mn^{3+}. For the $Ca_{1-x}(La/Ce)_xMnO_3$ systems, the temperature dependent ΔH_{PP} above T_N normally displays the relation to $(T - T_N)^{-P}$, which is substantially different from ΔH_{PP}(T) of the hole-doped manganites. Previous study concerning the electron-doped $La_{0.96}Te_{0.04}MnO_3$ shows that there is a PM phase below T_C due to the magnetic inhomogeneity but the temperature dependence of ΔH_{PP} and the intensity have not been studied. In this paper, we systematically investigate EPR spectra upon the different doping level of Te in a broad temperature range for the electron-doped manganites $La_{1-x}Te_xMnO_3$ ($0.1 \leq x \leq 0.2$). The results should provide a point of reference for an understanding of the EPR linewidth ΔH_{pp} above T_{min}, and is important to shed light on the debate regarding the behavior of $\Delta H_{PP}(T)$ and to correlate the results with different theoretical models.

2. Experiment

A ceramic sample of $La_{1-x}Te_xMnO_3$ ($0.1 \leq x \leq 0.2$) was synthesized by the conventional solid-state reaction starting with preheated La_2O_3 (99.99%), TeO_2 (99.9%) and MnO_2 (99.9%). The procedures of sintering and XRD characterization of the sample are described elsewhere.[16] EPR spectra were recorded using a X-band Bruker ELEXSYS E500 and EMXplus 10/12 cw spectrometer with 100 kHz magnetic field modulation within the temperature range of 120–400 K. EPR detects the power P absorbed by a sample from a transverse magnetic microwave field. The signal-to-noise ratio of the spectra can

[a] *Key Laboratory of Materials Physics, Institute of Solid State Physics, Chinese Academy of Sciences, Shushanhu Road 350, Hefei 230031, People's Republic of China. E-mail: jyang@issp.ac.cn*
[b] *Hefei National Laboratory for Physical Sciences at Microscale and Department of Modern Physics, University of Science and Technology of China, Hefei 230026, People's Republic of China*
[c] *Department of Experimental Physics III, Technische Universität Dortmund, Otto-Hahn-Straße 4, 44221 Dortmund, Germany*
[d] *High Magnetic Field Laboratory, Chinese Academy of Sciences, Hefei 230031, People's Republic of China. E-mail: ypsun@issp.ac.cn*

be improved by recording the first derivative of P (dP/dH) with a lock-in technique. The magnetic susceptibility was measured by a vibrating sample magnetometry (VSM). The resistance measurement was performed by the standard four-probe method.

3. Results and discussion

Fig. 1, 2, and 3 show the EPR spectra dP/dH at different temperatures for the samples with $x = 0.1$, 0.15, and 0.2, respectively. It can be seen from Fig. 1–3(a) that one single resonance line which has a Lorentzian shape is observed in the EPR spectra above 280, 290, and 280 K for the samples with $x = 0.1$, 0.15, and 0.2, respectively. The resonance field is centered at about 3300 Gauss and is independent of temperature. For the sample with $x = 0.1$, the lineshape of the signal becomes distorted lightly from 260 K and the resonance line cannot be well reproduced by the single Lorentzian shape function. With the temperature further decreasing to 240 K corresponding to the Curie temperature of $La_{0.9}Te_{0.1}MnO_3$ ($T_C = 239$ K), the whole resonance becomes distorted heavily. Moreover, the resonance line broadens and the resonance field gradually shifts to lower field due to the internal fields caused by the onset of magnetic order. The shape of this line is typical for ferromagnetic resonance (FMR) signal originating from the FM metal phase. For the samples with $x = 0.15$ and 0.2, the resonance lines exhibit similar behavior. It should be noted that absorption dip starts to occur around T_C of the samples at ~500 G, which is obvious for the $x = 0.15$ sample in the temperature range of 235–255 K. As an example, the inset

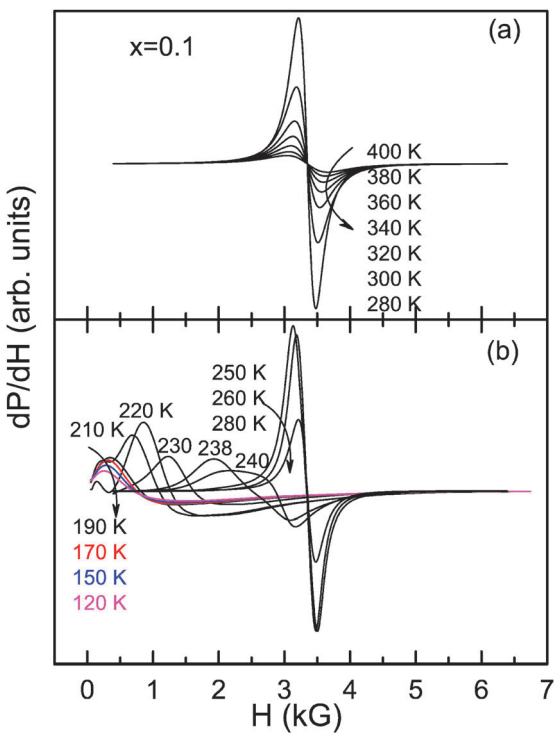

Fig. 1 EPR spectra of $La_{0.9}Te_{0.1}MnO_3$ at different temperatures: (a) from 280 to 400 K and (b) from 120 to 280 K. The repeat plot of 280 K in (b) is just for a guide to the eye for the change in the lineshape from 400 K to 120 K.

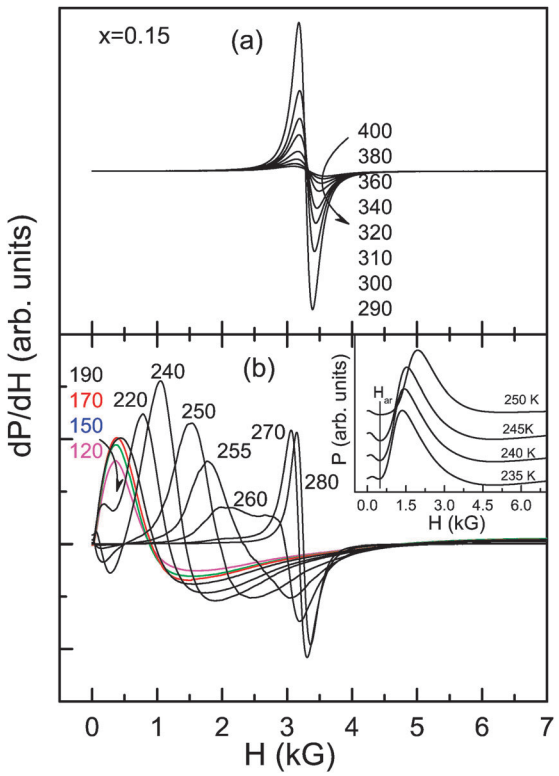

Fig. 2 EPR spectra of $La_{0.85}Te_{0.1}MnO_3$ at different temperatures: (a) from 290 to 400 K, and (b) from 120 to 280 K. The inset shows the absorption spectrum as a function of field. H_{ar} denotes the FMAR field.

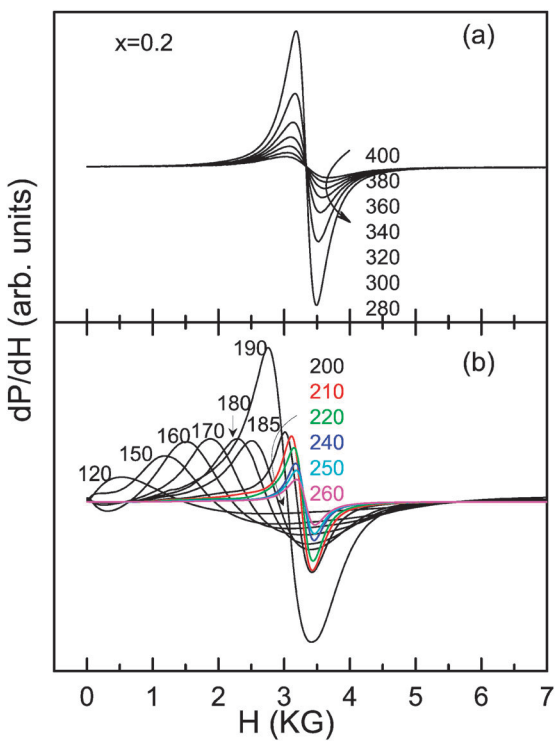

Fig. 3 EPR spectra of $La_{0.8}Te_{0.2}MnO_3$ at different temperatures: (a) from 280 to 400 K, and (b) from 120 to 260 K.

of Fig. 2 (b) shows the absorption spectrum as a function of field. The minimum of the spectra denotes the appearance of ferromagnetic antiresoance (FMAR),[17] which is often observed in the FM conductors in the case of the dimension of the measured samples being much smaller than the microwave skin depth.

In order to precisely determine the EPR parameters, *i.e.*, resonance field and linewidth, we have fitted the symmetric signals by the Lorentzian shape function:[18]

$$\frac{dP}{dH} = \frac{d}{dH}\left[\frac{2A}{\pi} \times \left(\frac{\Delta H_{\mathrm{FWHM}}}{4(H - H_r)^2 + \Delta H_{\mathrm{FWHM}}^2}\right)\right] \qquad (1)$$

where A denotes the area under the absorption curve, *i.e.*, EPR signal intensity, H_r is the resonance field and ΔH_{FWHM} is the Lorentzian full width at half maximum (FWHM) in the absorption curve. The peak-to-peak linewidth ΔH_{pp} can be obtained from the fit parameters ΔH_{FWHM} using $\Delta H_{pp} = \Delta H_{\mathrm{FWHM}}/\sqrt{3}$. The EPR spectra of the samples with $x = 0.1$, 0.15, and 0.2 above 280, 290, and 280 K, respectively, can be well described by eqn (1), whereas the discrepancy between the experimental data and the calculated ones occurs below these temperatures. As an example, the illustration of the fit results at the temperature of 280 K, 290 K, and 280 K for the samples with $x = 0.1$, 0.15, and 0.2, respectively, are shown by the solid lines in Fig. 4(a). Below these temperatures, *i.e.*, at $T = 250$–270 K for the $x = 0.1$ sample, at $T = 265$–280 K for the $x = 0.15$ sample, and at $T = 200$–260 K for the $x = 0.2$ sample, we use the second derivative d^2P/dH^2 curve to determine the linewidth due to the asymmetric and distorted resonance lines, *e.g.*, the appearance of a shoulder marked by the triangular symbol as shown in Fig. 4(b).

Fig. 5(a) and (b) show the best fit to the spectrum at some typical temperatures for the $x = 0.15$ and $x = 0.2$ samples, respectively. It is found that just below the temperature of the appearance of a single PM resonance line, the resonance signals can be fitted well by the superposition of two Lorentzian-shape lines. One line located at the resonance field of $\sim$3000 G denotes the PM resonance signal and the other represents the FM resonance signal. With the temperature is lowered towards T_C, the spectrum can be well fitted by three inhomogeneously-broadened Gaussian lines, which is in agreement with the fact that the resonance lines often approach the Gaussian shape if the line is a superposition of many components.[18] The three lines develops and shifts to lower field with decreasing temperature. As the temperature is lower than T_C, the spectrum gradually transforms into a single FM resonance line. The appearance of the FM signal well above the Curie temperature ($T_C = 241$ K for the $x = 0.15$ sample and $T_C = 189$ K for the $x = 0.2$ sample) implies that the magnetic state of the samples are of magnetic inhomogeneity or phase separated consisting of two distinguished magnetic phases, which will be discussed in more detail later.

Fig. 6(a) shows the temperature dependence of the EPR linewidth ΔH_{pp} for the samples with $x = 0.1$, 0.15, and 0.2. There is a minimum at T_{min} for all the samples on the plot of ΔH_{pp}(T). It is interesting that T_{min} corresponds to the temperature below which some distortions of the lineshape occur.

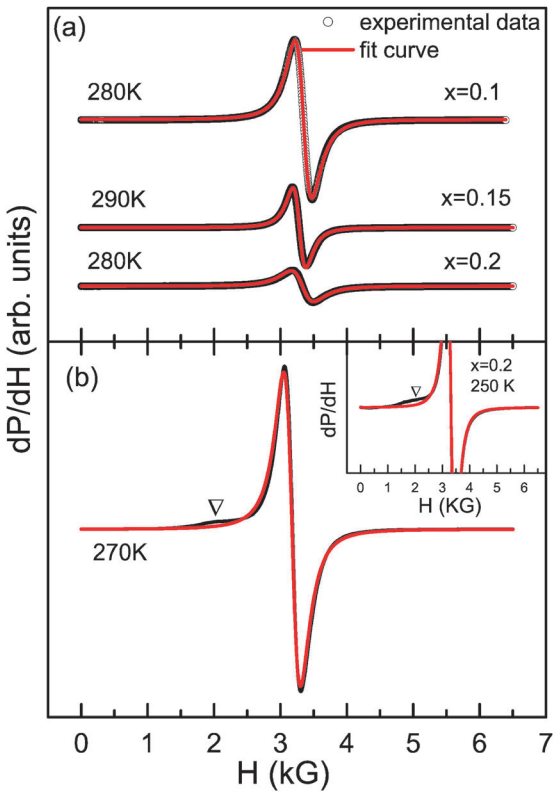

Fig. 4 The experimental EPR spectra and the fit curve (shown by the solid lines) of the samples according to eqn (1) at (a) temperatures above which only one symmetric PM resonance line exists, and (b) 270 K for the $x = 0.15$ sample. The inset shows the enlarge plot of the $x = 0.2$ sample at 250 K. The triangular symbol denotes the distortion of the lines implying the appearance of FM resonance signals.

The difference between T_{min} and T_C may be due to some magnetic inhomogeneity in materials.[4] This can be further confirmed by the temperature dependence of inverse dc magnetic susceptibility ($1/\chi = H/M$). The inset of Fig. 6(a) shows the temperature dependence of the $1/\chi$ for the samples. The solid lines are the calculated curve deduced from the Curie–Weiss equation. It can be seen that the experimental curves above 240 K ($T_C = 239$ K), 250 K ($T_C = 241$ K), and 200 K ($T_C = 189$ K) for the samples with $x = 0.1$, 0.15, and 0.2, respectively, can be well described by the Curie–Weiss law indicating the absence of the short-range magnetic correlations and the existence of a pure PM state above these temperatures for the samples. However, from the EPR spectra and the plot of ΔH_{pp}(T), we believe that the real PM state exists only above T_{min}. Between T_C and T_{min}, FM clusters with short-range ordering exist in a PM matrix. The results indicate that EPR is a very effective tool to probe the local and microscopic magnetic states compared to the mere magnetic measurements. Moreover, it is found that the linewidth of the $x = 0.1$ sample in the PM region is between that of the $x = 0.15$ and 0.20 sample, which is due to the difference in the magnitude of spin–lattice interaction. For the $x = 0.2$ sample, the spin–lattice interaction is stronger due to its lower T_C, and thus the spin–lattice relaxation time (T_1) is shorter giving rise to the rather large linewidth compared to the $x = 0.1$ and 0.15 sample.

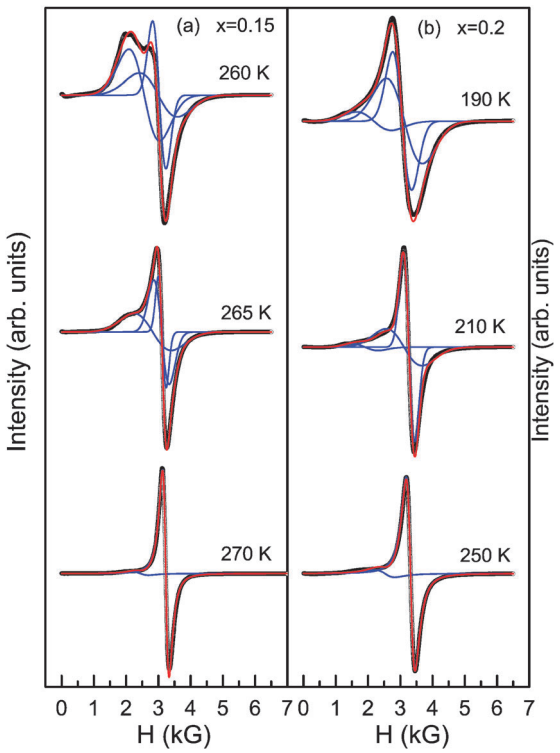

Fig. 5 The EPR spectra at some typical temperatures for (a) the $x = 0.15$ sample, and (b) the $x = 0.2$ sample. The scattered points are the experimental data and the solid line superimposed on it denotes the fit curve. Other solid lines represent the decomposed component.

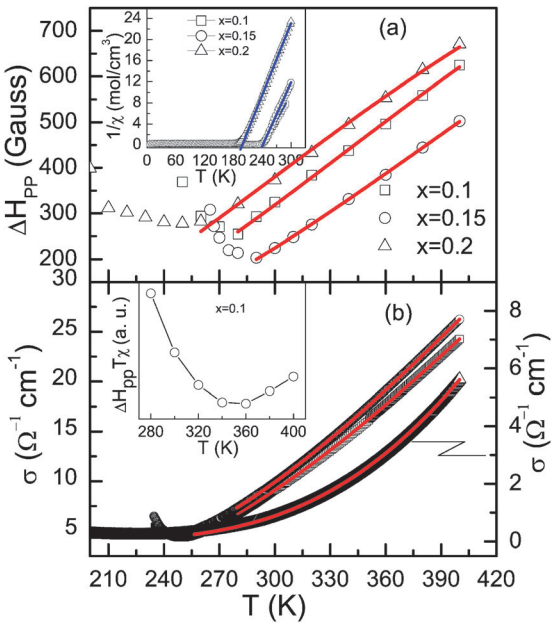

Fig. 6 (a) Temperature dependence of the EPR linewidth ΔH_{PP}. The error bars are much smaller than the symbols (not shown). The solid lines denote the best fit to the linewidth data above T_{min} based on eqn (2). The inset shows the temperature dependence of $1/\chi$ for the samples. The lines are the calculated curves according to the Curie–Weiss law. (b) The conductivity as a function of temperature. The solid line denotes the fit according to the small polaron hopping model. The inset shows the temperature dependence of the product $\Delta H_{PP} T\chi$ for the $x = 0.1$ sample.

In the following we discuss the temperature dependence of the EPR linewidth ΔH_{pp} above T_{min}. In the real PM region, the EPR linewidth can be well described by the expression:

$$\Delta H_{pp}(T) \propto \frac{A}{T}\exp(-E_a/k_B T) \qquad (2)$$

where A is a constant, E_a is the activation energy, and k_B is Boltzmann's constant. The solid lines in Fig. 6(a) represent the best fit to the data using the expression and the activation energy can thus be obtained as 0.0987(13), 0.1128(6), and 0.0874(14) eV for the samples with $x = 0.1$, 0.15, and 0.2, respectively. It is well known that the conductivity σ of manganites in the paramagnetic regime is dominated by the adiabatic hopping motion of small polarons. Moreover, the proportionality between the EPR linewidth and the conductivity is often observed in systems with hopping conductivity.[19] Therefore, we also plotted the temperature dependence of the conductivity for the samples in Fig. 6(b). The solid lines denote the fit data above T_{min} by a small-polaron hopping model (SPH) $\sigma \propto \frac{A}{T}\exp(-E_\sigma/k_B T)$, where E_σ is the activation energy. The results show that $\sigma(T)$ curves above T_C can be well described by SPH model and thus the obtained activation energy is 0.1312(4), 0.1305(4), and 0.2206(2) eV for the samples with $x = 0.1$, 0.15, and 0.2, respectively. The observed similarity between temperature dependencies of the EPR linewidth and the conductivity indicates that the energy transfer in the relaxation mechanism could be provided by the thermally activated hopping of small e_g polarons. Furthermore, this similarity arises from the fact that the hopping rate of the charge carriers will determine the lifetime of spin state and thus the EPR linewidth, as well as the conductivity.[20] For the manganites system, the charge carriers are e_g electrons. As a result, the hopping of e_g electrons from Mn^{2+} to Mn^{3+} *via* the neighboring O ions in $La_{0.9}Te_{0.1}MnO_3$will determine the EPR linewidth. Within this scenario, the variation of E_σ upon the doping level of $La_{1-x}Te_xMnO_3$ can be understood in terms of the different magnitude of lattice distortion. It is known that the lattice distortion will lower the mobility of e_g electrons and therefore assists localization of polarons that is directly related to the activation energy of the sample. For the $x = 0.2$ sample, the stronger lattice distortion corresponding to a lower Mn–O–Mn bond angle ($\theta_{Mn-O-Mn} = 162.24$)[21] will lead to the higher activation energy compared to the $x = 0.1$ sample ($\theta_{Mn-O-Mn} = 163.81$) and the $x = 0.15$ sample ($\theta_{Mn-O-Mn} = 163.83$).[21] Moreover, It is found that for the samples with $x = 0.1$ and 0.15, the value of E_σ is comparable with that of activation energy deduced from the EPR linewidth data. Whereas for the $x = 0.2$ sample, it is worthwhile to note that there is a large difference between the activation energies obtained from the resistivity (0.2206 eV) and the linewidth (0.0874 eV). The difference in the E_a and E_σ values are also observed in some hole-doped manganites.[22,23] The hopping of e_g polarons will decrease Hund's rule correlations between the core spins and e_g polarons. And this correlation will diminish with decreasing/increasing $\theta_{Mn-O-Mn}/d_{Mn-O}$ leading to the large differences in E_a and E_σ.

A considerable amount of controversy exists regarding the interpretation of the ΔH_{PP} dependent on temperature for

$T \geq T_{min}$ and the mechanisms are mainly as follows: (a) the combination of exchange-narrowing spin–spin interaction and spin–lattice interaction,[8] (b) a spin-only relaxation mechanism resulting in a universal quasilinear temperature dependence of the linewidth,[5] (c) a spin-phonon interaction proposed by Seehra *et al.*[2] and (d) the bottlenecked spin relaxation from the exchange-coupled constituent Mn^{4+} ions *via* the Mn^{3+} Jahn–Teller ions to the lattice.[1] In model (a), the EPR linewidth can be described by the formula $\Delta H_{pp} = \Delta H_{pp,min} + b(T - T_{min})$. The first term and second term is related to the exchange-narrowing spin–spin interaction and the spin–lattice interaction, respectively. Moreover, it was shown that the product $\Delta H_{pp,min} T_C$ almost keeps constant for the samples with different ionic radius of A-site ions $\langle r_A \rangle$. According to this model, we can deduce the value of $\Delta H_{pp,min}$ as 400 Gauss for $La_{0.9}Te_{0.1}MnO_3$ and this calculation value is obviously larger than 250 Gauss from the experimental data. Therefore, model (a) is not valid for the present system $La_{0.9}Te_{0.1}MnO_3$. Additionally, a clear deviation from the quasilinear behavior of ΔH_{PP} (T/T_C) *vs.* ΔH_{PP} (∞) proposed by Causa *et al.* (model (b)) was observed for the samples (not shown here). Therefore, both model (a) and (b) are not valid for the present system $La_{0.9}Te_{0.1}MnO_3$. In model (c), Seehra *et al.* explained a linear dependence of linewidth in manganites[2] and the linewidth can be written as $\Delta H = \frac{\hbar[c + f(\varepsilon)]}{g\mu_B T\chi_0}$, where μ_B is the Bohr magneton, $\hbar$ is Planck's constant, $f(\varepsilon)$ is the critical contribution to ΔH from spin–spin interactions which is significant only for $\varepsilon = (T - T_C)/T_C \leq 0.1$ for $T \approx T_C$ and c is the non-critical contribution from spin-phonon interactions for $T \gg T_C$. If there is no contribution to the linewidth from spin-phonon interactions, the product $\Delta H T\chi_0$ would approach a temperature independent constant value for $T \gg T_C$. The spin–phonon contribution to ΔH may vary as T or T^2 depending on whether one-phonon or two-phonon contributions are dominant. Actually, model (d) also covers the spin-phonon (vibrations of the lattice) or spin–lattice interactions.

In order to check if there is the contribution of spin–lattice interaction to the temperature dependence of ΔH_{PP}, we plot the product $\Delta H_{PP} T\chi$ as a function of temperature above T_{min} for the $x = 0.1$ sample. It can be seen from the inset of Fig. 6(b) that the product $\Delta H_{PP} T\chi$ is not a constant and is temperature dependent implying a contribution of the spin–lattice interaction to the ΔH_{PP} for $La_{0.9}Te_{0.1}MnO_3$. From the aforementioned analysis, we can understand the reason for the broadening of the EPR linewidth above T_{min} for the samples. It was shown that increasing temperature can enhance the thermal motion of the lattice so that it is favorable for the spin system to exchange energy leading to the decrease of the spin–lattice relaxation time T1 and thus the broadening of the EPR line. In other words, the broadening of the EPR line arises from the increase in the spin–lattice relaxation rate with increasing temperature.

It seems that the features of the T-dependent linewidth $\Delta H_{PP}(T)$, *i.e.*, with decreasing temperature, ΔH_{PP} decreases, passes through a minimum at T_{min} and then substantially increases on further decreasing temperature, are similar between the hole-doped and electron-doped manganites. This may be related to the analogous electronic structure for the hole-doped and electron-doped manganites. Note that Mn^{3+} is a Jahn–Teller ion, Mn^{4+} and Mn^{2+} are both non Jahn–Teller ions. Thus, the basic physics in terms of Hund's rule coupling and Jahn–Teller effect could operate in the electron-doped phase as well.

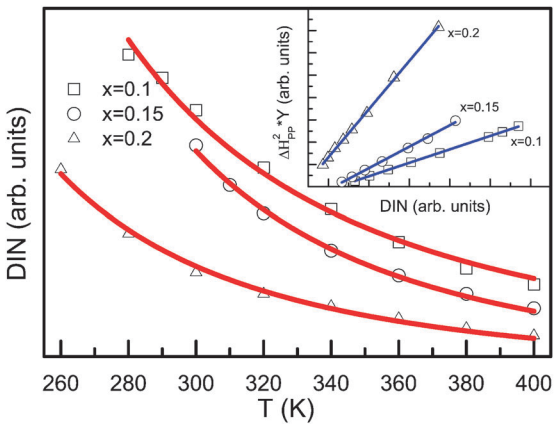

Fig. 7 The double integration intensity of EPR spectra as a function of temperature. The error bars are much smaller than the symbols (not shown). The solid line represents the fit based on Arrhenius law. The inset shows the product $(\Delta H_{pp})^2 Y'$ scales with DIN and the solid lines are the linear fit.

The intensity of EPR spectra is used to identify the nature of the magnetic ions contributing to the resonance which can be proportional to the number of spins, and it is normally determined in two ways: (a) by numerical double integration of the recorded dP/dH spectra, and (b) approximately the area by the product$(\Delta H_{pp})^2 Y'$, where $2Y'$ is the peak-to-peak derivative amplitude. Both methods gave results proportional to each other as seen from the inset of Fig. 4. Here we use the double integration (DIN) of observed EPR spectra for the following discussion. It should be noted that meaningful integration requires a base-line correction after each integration, so there has to be good base line on the low-field and high-field sides of the spectrum. The DIN is found to decrease exponentially as the temperature increases as shown in Fig. 7. The DIN of the EPR spectra during the PM regime for many manganite is usually described by the Arrhenius law:[5] $DIN = I_0 \exp(\Delta E/K_B T)$, where ΔE is the activation energy for dissociation of the paramagnetic spin clusters. It is necessary to note that the Arrhenius exponential law could be deduced at the frame of SPH model when the ESR linewidth as a function of temperature is proportional to the electrical conductivity.[5] The Arrhenius plot of the intensity above 280 K, 300 K, and 260 K for the samples with $x = 0.1$, 0.15, and 0.2, respectively, is shown by the solid line in Fig. 7. It is seen that the DIN obeys the law well with ΔE of 0.0942(62), 0.1189(49), and 0.0963(29) eV for the samples with $x = 0.1$, 0.15, and 0.2, respectively, which is very close to the activation energy deduced from the temperature dependence of the EPR linewidth ΔH_{pp}.

4. Conclusions

In summary, we measured the EPR spectra at different temperatures for the electron-doped manganite $La_{1-x}Te_xMnO_3$ $(0.1 \leq x \leq 0.2)$. Together with the temperature dependence of the linewidth $\Delta H_{pp}(T)$ and inverse magnetic susceptibility $1/\chi$,

we believe that a real PM region exist above T_{min}. Between T_C and T_{min}, a short-range FM ordering appears in a PM matrix. Both the EPR linewidth ΔH_{pp}(T) above T_{min} and conductivity $\sigma(T)$ above T_{I-M} follow the small polarons hopping model with a similar value of the activation energy. Further analysis indicates that the broadening of the EPR line arises from the increase in the relaxation rate of spin of e_g polarons to the lattice with increasing temperature. For the sample with $x = 0.2$, there is a large difference between the conductivity activation energy E_σ and the activation energy E_a deduced from the linewidth arising from the decrease in Hund's rule correlations.

Acknowledgements

J. Yang acknowledges support by the Alexander von Humboldt Foundation, and thanks Dr W. Tong for the help in the EPR measurements. The author Y. P. Sun acknowledges support by the National Key Basic Research under Contract No. 2007CB925002, the National Science Foundation of China under Contract Nos.10774146, and 10904150.

References

1 A. Shengelaya, G. M. Zhao, H. Keller and K. A. Müller, *Phys. Rev. Lett.*, 1996, **77**, 5296.
2 M. S. Seehra, M. Ibrahim, V. S. Babu and G. Srinivasan, *J. Phys.: Condens. Matter*, 1996, **8**, 11283.
3 S. B. Oseroff, M. Torikachvili, J. Singley, S. Ali, S.-W. Cheong and S. Schultz, *Phys. Rev. B: Condens. Matter*, 1996, **53**, 6521.
4 S. E. Lofland, P. Kim, P. Dahiroc, S. M. Bhagat, S. D. Tyagi, S. G. Karabashev, D. A. Shulyatev, A. A. Arsenov and Y. Mukovskii, *Phys. Lett. A*, 1997, **233**, 476.
5 M. T. Causa, M. Tovar, A. Caneiro, F. Prado, G. Ibanez, C. A. Ramos, A. Butera, B. Alascio, X. Obradors, S. Pinol, F. Rivadulla, C. Vazquez-Vazquez, A. Lopez-Quintela, J. Rivas, Y. Tokura and S. B. Oseroff, *Phys. Rev. B: Condens. Matter*, 1998, **58**, 3233.
6 D. L. Huber, G. Alejandro, A. Caneiro, M. T. Causa, F. Prado, M. Tovar and S. B. Oseroff, *Phys. Rev. B: Condens. Matter*, 1999, **60**, 12155.
7 F. Rivadulla, M. A. Lopez-Quintela, L. E. Hueso, J. Rivas, M. T. Causa, C. A. Ramos, R. D. Sanchez and M. Tovar, *Phys. Rev. B: Condens. Matter*, 1999, **60**, 11922.
8 S. L. Yuan, G. Li, Y. jiang, J. Q. Li, X. Y. Zeng, Y. P. Yang, Z. Huang and S. Z. Jin, *J. Phys.: Condens. Matter*, 2000, **12**, L109.
9 V. A. Ivanshin, J. Deisenhofer, H.-A. Krug von Nidda, A. Loidl, A. A. Mukhin, A. M. Balbashov and M. V. Eremin, *Phys. Rev. B: Condens. Matter*, 2000, **61**, 6213.
10 J. P. Joshi, R. Gupta, A. K. Sood, S. V. Bhat, A. R. Raju and C. N. R. Rao, *Phys. Rev. B: Condens. Matter*, 2001, **65**, 024410.
11 A. N. Ulyanov, S. C. Yu, S. G. Min and G. G. Levchenko, *J. Appl. Phys.*, 2002, **91**, 7926.
12 S. Angappane, M. Pattabiraman, G. Rangarajan, K. Sethupathi, B. Varghese and V. S. Sastry, *J. Phys.: Condens. Matter*, 2007, **19**, 036207.
13 G. T. Tan, S. Dai, P. Duan, Y. L. Zhou, H. B. Lu and Z. H. Chen, *Phys. Rev. B: Condens. Matter*, 2003, **68**, 014426.
14 E. Granado, N. O. Moreno, H. Martinho, A. García, J. A. Sanjurjo, I. Torriani, C. Rettori, J. J. Neumeier and S. B. Oseroff, *Phys. Rev. Lett.*, 2001, **86**, 5385.
15 A. Sharma, S. Sarangi and S. V. Bhat, *Phys. Rev. B: Condens. Matter Mater. Phys.*, 2006, **73**, 035129.
16 J. Yang, W. H. Song, Y. Q. Ma, R. L. Zhang, B. C. Zhao, Z. G. Sheng, G. H. Zheng, J. M. Dai and Y. P. Sun, *Phys. Rev. B: Condens. Matter Mater. Phys.*, 2004, **70**, 144421.
17 S. M. Bhagat, in *Techniques of Metal Research*, ed. E. Passaglia, Interscience, New York, 1974, vol. VI, Part 2, ch. 8.
18 John A. Weil and James R. Bolton, in *Electron Paramagnetic Resonance: Elementary Theory and Practical Applications*, John Wiley & Sons, Inc., Hoboken, New Jersey, 2nd edn, 2007.
19 O. Chauvet, T. Stoto and L. Zuppiroli, *Phys. Rev. B: Condens. Matter*, 1992, **46**, 8139.
20 B. Movaghar and L. Schweitzer, *Philos. Mag.*, 1978, **37**, 683.
21 J. Yang, W. H. Song, Y. Q. Ma, R. L. Zhang, B. C. Zhao, Z. G. Sheng, G. H. Zheng, J. M. Dai and Y. P. Sun, *Mater. Chem. Phys.*, 2005, **94**, 62.
22 S. K. Misra, S. I. Andronenko, S. Asthana and D. Bahadur, *J. Magn. Magn. Mater.*, 2010, **322**, 2902.
23 V. Markovich, I. Fita, A. I. Shames, R. Puzniak, E. Rozenberg, C. Martin, A. Wisniewski, Y. Yuzhelevskii, A. Wahl and G. Gorodetsky, *Phys. Rev. B: Condens. Matter*, 2003, **68**, 094428.

